THE JOURNAL OF BIOLOGICAL CHEMISTRY
Vol. 279, No. 10, Issue of March 5, pp. 9547–9556, 2004
Printed in U.S.A.

Kinetic Interaction Analysis of Human Interleukin 5 Receptor α Mutants Reveals a Unique Binding Topology and Charge Distribution for Cytokine Recognition*

Received for publication, August 22, 2003, and in revised form, November 6, 2003
Published, JBC Papers in Press, December 7, 2003, DOI 10.1074/jbc.M309327200

Tetsuya Ishino‡, Gianfranco Pasut§, Jeffery Scibek‡, and Irwin Chaiken‡¶

From the ‡Biochemistry Department and A. J. Drexel Institute of Basic and Applied Protein Science, College of Medicine, Drexel University, Philadelphia, Pennsylvania 19102 and the §Pharmaceutical Sciences Department, University of Padua, Padua 35121, Italy

Human interleukin 5 receptor α (IL5Rα) comprises three fibronectin type III domains (D1, D2, and D3) in the extracellular region. Previous results have indicated that residues in the D1D2 domains are crucial for high affinity interaction with human interleukin 5 (IL5). Yet, it is the D2D3 domains that have sequence homology with the classic cytokine recognition motif that is generally assumed to be the minimum cytokine-recognizing unit. In the present study, we used kinetic interaction analysis of alanine-scanning mutational variants of IL5Rα to define the residues involved in IL5 recognition. Soluble forms of IL5Rα variants were expressed in S2 cells, selectively captured via their C-terminal V5 tag by anti-V5 tag antibody immobilized onto the sensor chip and examined for IL5 interaction by using a sandwich surface plasmon resonance biosensor method. Marked effects on the interaction kinetics were observed not only in D1 (Asp^{55}, Asp^{56}, and Glu^{58}) and D2 (Lys^{186} and Arg^{188}) domains, but also in the D3 (Arg^{297}) domain. Modeling of the tertiary structure of IL5Rα indicated that these binding residues fell into two clusters. The first cluster consists of D1 domain residues that form a negatively charged patch, whereas the second cluster consists of residues that form a positively charged patch at the interface of D2 and D3 domains. These results suggest that the IL5·IL5Rα system adopts a unique binding topology, in which the cytokine is recognized by a D2D3 tandem domain combined with a D1 domain, to form an extended cytokine recognition interface.

Interleukin 5 (IL5)[1] is a T cell-derived cytokine that plays a central role in maturation and proliferation of eosinophils (1). IL5 exerts biological functions through recruitment of a cell surface receptor composed of two polypeptide chains (2), α and β. The α chain is IL5-specific and is called IL5 receptor α (IL5Rα), whereas the β chain is shared with IL3 and GM-CSF (3, 4) and is called common β chain (βc). The α chains for IL3, GM-CSF, and IL5Rα also share a high degree of amino acid sequence similarity and constitute a distinct subgroup within the cytokine receptor family (5). Because IL5 has been implicated in the pathology of eosinophil-related inflammatory diseases, designing specific antagonists for IL5Rα may offer therapeutic benefits in the treatment of such diseases (6, 7).

IL5 initially binds to IL5Rα with high affinity, and the resulting complex recruits βc to induce cytoplasmic signal transduction. Human IL5Rα alone binds IL5 with an equilibrium dissociation constant (K_d) of 0.3–0.6 nM when expressed in COS cells (8). The binding affinity is increased only 2- to 5-fold when human α and β chains are co-expressed (3). In other words, IL5Rα provides most of the IL5 binding energy, whereas βc is essentially for signaling. IL5Rα consists of an extracellular region, a single transmembrane region and a cytoplasmic region. A soluble form of IL5Rα (sIL5Rα) containing only the extracellular region was cloned and expressed (9). This form has provided a convenient tool for biochemical and biophysical characterizations of the receptor, showing that stoichiometry of interaction between IL5 and IL5Rα is 1:1, and the K_d value is 0.6 nM (10) or 2–5 nM (11, 12) depending on the assay method.

Extensive studies have been carried out on human IL5 to identify epitopes important for receptor α and βc recruitment. Crystallographic analysis has revealed that IL5 is a symmetric homodimer in which each helical bundle domain is composed of three helices (A–C) from one chain and one (D) from the other (13). Site-directed mutagenesis analyses have shown the importance of charged residues in helix B (His^{38}, Lys^{39}, and His^{41}), CD turn (Glu^{88}, Glu^{89}, Arg^{90}, and Arg^{91}), and helix D (Glu^{110}) for IL5Rα binding (14–16). Moreover, phage-based CD turn randomization (17) has led to identification of a functionally active IL5 mimetic containing the CD turn sequence ^{88}SLRGG^{92}, instead of the native sequence ^{88}EERRR^{92}. In the CD turn of this IL5 mutant, the only charged residue is the Arg^{90}. Regarding βc binding epitope, Glu^{13} in helix A is thought to be a key residue for βc recruitment (16).

On the other hand, structure-function relationships for IL5Rα are less delineated. IL5Rα is a member of the class I cytokine receptor superfamily (18), which is characterized by the presence of the so-called cytokine recognition motif (CRM). The CRM is composed of two fibronectin type III (FnIII) domains, each consisting of ~100 residues with four conserved Cys residues in the first FnIII domain and a conserved WS*X*WS (Trp-Ser-*X*-Trp-Ser, where *X* is any amino acid residue) sequence in the second FnIII domain. The FnIII domain forms a β-sandwich where seven β-strands (A–G) are arranged in the Greek key topology. As found in immunoglobulin (Ig) folds, the β-sheet of FnIII is folded between strands D and E. In the first

* This work was supported by National Institutes of Health Grants GM55648 and AI40462. The costs of publication of this article were defrayed in part by the payment of page charges. This article must therefore be hereby marked "*advertisement*" in accordance with 18 U.S.C. Section 1734 solely to indicate this fact.

¶ To whom correspondence should be addressed: Biochemistry Department and A. J. Drexel Institute of Basic and Applied Protein Science, Drexel University College of Medicine, 11102 New College Building, MS# 497, 245 N. 15th Street, Philadelphia, PA 19102. Tel.: 215-762-4197; Fax: 215-762-4452; E-mail: imc23@drexel.edu.

[1] The abbreviations used are: IL5, interleukin 5; IL5Rα, interleukin 5 receptor α chain; sIL5Rα, soluble form of IL5Rα; GM-CSF, granulocyte/macrophage-colony-stimulating factor; CRM, cytokine recognition motif; FnIII, fibronectin type III; RU, resonance unit(s).

FnIII domain of CRM, one disulfide bond links the neighboring strands A and B and another disulfide bond links strands D and E, cross-linking the two sheets of the sandwich. The WS*X*WS sequence is located between strands F and G in the second FnIII domain and plays a structural role in correctly positioning the second domain (19). There are two kinds of domain architecture in the class I cytokine receptor superfamily: one consists of a single CRM, like growth hormone, erythropoietin, and IL4 receptors; another contains extra FnIII and/or Ig-like domains in addition to one or more sets of CRM, like gp130, IL12 p70, and granulocyte colony-stimulating factor receptor. In either case, it is a general rule that a cytokine is recognized by its receptor CRM. Structures of complexes of these receptors have been solved using x-ray crystallography, demonstrating that the two FnIII domains of CRM form an L shape, and a cytokine is bound to the elbow region, which is constituted by several loops connecting the β-strands (reviewed in Ref. 20). As Bazan has proposed (18), the conserved residues in CRM appear to contribute to a skeletal framework, which would be enriched by cytokine-specific residues in these loops.

The extracellular region of IL5Rα is composed of three FnIII domains, D1, D2, and D3 (domain numbering from the N terminus). Previously, chimeric and site-directed mutagenesis analyses have demonstrated the importance of D1D2 domains, in which Asp^{55}, Asp^{56}, Tyr^{57}, Glu^{58}, and Arg^{188} residues play a crucial role in the specific interaction of IL5Rα with IL5 (21). However, this previous mutagenesis was not targeted to elucidate the entire binding sites on IL5Rα molecule. Indeed, it is the D2D3 domains that have sequence homology with the classic CRM that is assumed to be the minimum cytokine-recognizing unit. From these standpoints, a wider-ranging binding site analysis seemed potentially useful to more fully elucidate the IL5 recognition mechanism of IL5Rα. A major starting point of this work was the realization that electrostatic interactions may be dominant in the IL5·IL5Rα system, because the important binding residues on the human IL5 molecule are mostly charged amino acids, and some residues already identified in IL5Rα as important for IL5 binding also are charged. In the present study, therefore, we selected 43 charged amino acid resides from D1, D2, and D3 domains of human IL5Rα for site-directed mutagenesis. We performed kinetic interaction analysis of alanine-scanning mutational variants of sIL5Rα in an attempt to expand the definition of the mechanism of molecular recognition of the IL5·IL5Rα interaction. Mutations that diminished the high affinity binding were found to be located in the D3 (Arg^{297}) domain as well as in D1 (Asp^{55}, Asp^{56}, and Glu^{58}) and D2 (Lys^{186} and Arg^{188}) domains. Kinetic analysis demonstrated that mutagenic changes of Asp^{55} and Arg^{188} appear to have the greatest impact on the fast association rate of IL5·IL5Rα interaction. The effects of mutation can be rationally interpreted in terms of tertiary structure. The homology-deduced IL5Rα structure indicated that the IL5 binding interface of receptor α comprises a cluster of negatively charged residues from D1 domain and a cluster of positively charged residues from D2D3 domains. Together, the results suggest the possibility that the IL5·IL5Rα system adopts a unique interaction topology, in which the cytokine is recognized by a D1 domain and a D2D3 tandem domain.

EXPERIMENTAL PROCEDURES

Materials—Human IL5 protein was prepared as described previously (22). The anti-human IL5Rα monoclonal antibody, α16 (23), was a generous gift from Dr. J. Tavernier (University of Ghent, Ghent, Belgium). All the enzymes were purchased from New England Biolabs Inc. (Beverly, MA). All the oligonucleotide DNA primers, anti-V5 tag monoclonal antibody, *Drosophila* Schneider 2 (S2) cells, cell culture media, and L-glutamine solution (200 mM) were purchased from Invitrogen Inc. (Carlsbad, CA). For surface plasmon resonance measurements, the sensor chip CM5, surfactant P20, *N*-ethyl-*N*-(3-dimethylaminopropyl)carbodiimide, *N*-hydroxysuccinimide, 1 M ethanolamine (pH 8.5), and 10 mM glycine-HCl (pH 1.5) were purchased from Biacore Inc. (Piscataway, NJ).

S2 Cell Expression of IL5Rα and Mutagenesis—pMTAL-IL5Rα (12) was used as a PCR template for generating a DNA fragment containing the soluble form of human IL5Rα (sIL5Rα). The PCR product was digested with NcoI and ApaI and ligated into the NcoI and ApaI sites of the *Drosophila* expression vector, pMT/Bip/V5-His A plasmid (Invitrogen), yielding pMT-sIL5Rα-V5-His. In this construct, the gene for sIL5Rα was placed behind the *Drosophila* metallothionein promoter and the Bip secretion signal sequence. The C terminus of sIL5Rα was linked to a V5 epitope sequence and a hexahistidine sequence (Fig. 1*A*). The amino acid sequence of final product is RSPW-sIL5Rα_{1-315}-GPFEGKPIPNPLLGLDSTRTGHHHHHH (V5 epitope sequence is underlined). For the alanine substitution variants, mutations were introduced into pMT-IL5Rα-V5-His using a QuikChange site-directed mutagenesis kit (Stratagene). Presence of the desired mutations was verified by DNA sequencing. Mutation sites are shown in Fig. 1*B*. Each plasmid was amplified in DH5α cells and purified for the subsequent transient transfection by using an S.N.A.P. midi prep kit (Invitrogen).

Drosophila S2 cells were transfected with the vector pMT-IL5Rα-V5-His using Cellfectin reagent (Invitrogen) and grown in serum-free medium supplemented with 20 mM L-glutamine. Protein expression was induced by addition of 600 μM copper sulfate 3 days after transfection. Cell-free supernatant was collected after 2 days and stored at −20 °C for the following binding analysis. The same procedure was used to obtain mutant proteins. Levels of expression were measured for both cell cultures and precipitants by Western blot using anti-human IL5Rα polyclonal antibody (R&D Systems) and anti-histidine tag polyclonal antibody (Santa Cruz Biotechnology). To obtain the precipitants, cells were lysed using CytoBuster (Novagen) and centrifuged 5 min at 15,000 × *g*.

Surface Plasmon Resonance Interaction Analysis—The kinetic interaction assay was performed using a Biacore 3000 optical biosensor (Biacore Inc., Uppsala, Sweden). All the experiments were conducted at 25 °C in phosphate-buffered saline buffer (1 mM KH_2PO_4, 10 mM Na_2HPO_4, 137 mM NaCl, 2.7 mM KCl, pH 7.4) with 0.005% P20.

Immobilization of antibodies on a CM5 sensor chip was carried out according to the standard protocol of the amine coupling method (BIAapplication handbook; Biacore). Briefly, ~1 mg/ml protein solution was diluted 100 times in 10 mM acetate (pH 4.5) and injected onto a biosensor surface that had been pre-activated with a 1:1 mixture of 200 mM *N*-ethyl-*N*-(3-dimethylaminopropyl)carbodiimide and 50 mM *N*-hydroxysuccinimide, followed by the injection of 1 M ethanolamine-HCl (pH 8.5). Flow cell 1 was used to immobilize 17b (anti-human immunodeficiency virus gp120 monoclonal antibody (24)) as a negative control, whereas the other three flow cells were used to immobilize, respectively, anti-V5 tag monoclonal antibody (Invitrogen), α16 (non-neutralizing anti-human IL5Rα monoclonal antibody (23)), and 2B6R (non-neutralizing anti-human IL5Rα monoclonal antibody (22)). Typically, the amounts of immobilization were around 2000 resonance units (RUs).

The expressed sIL5Rα was captured tightly by the antibodies immobilized on flow cells 2–4. On the other hand, other cell culture components passed through the sensor chip flow cells without binding (analogously as one would expect for affinity chromatography or other affinity capture). Subsequently, the real-time interaction of IL5 with the antibody-captured sIL5Rα was measured without detecting the large bulk effect caused by the cell culture components. To regenerate chip surfaces, both captured and bound proteins were removed from the antibody surfaces with 10 mM glycine-HCl, pH 1.5. For this sensor assay, all procedures were automated to create repetitive cycles of injection of cell-free culture (10 μl/min), 0–50 nM of IL5 (50 μl/min), and the regeneration buffer (100 μl/min). Injection time for the variants was varied to achieve a similar extent of capturing (300–600 RU, depending on the experiment). For the low-affinity variants (D55A, D56A, and R188A), the binding assay was repeated using up to 250 nM IL5.

Non-linear least-squares analysis was used to calculate the association and dissociation rate constants (k_{on} and k_{off}, respectively). Prior to the calculation, the binding data were corrected for nonspecific interaction by subtracting the negative control surface data (flow cell 1) from the reaction surface data (flow cells 2–4) and further corrected for buffer effect by subtracting the signal from buffer injections from those of protein sample injections (double referencing (25)). The interaction curves thus obtained were globally fit using a model for Langmuir 1:1 binding with mass transfer (BIAevaluation software, Biacore). The equilibrium dissociation constant K_d was calculated as $K_d = k_{off}/k_{on}$.

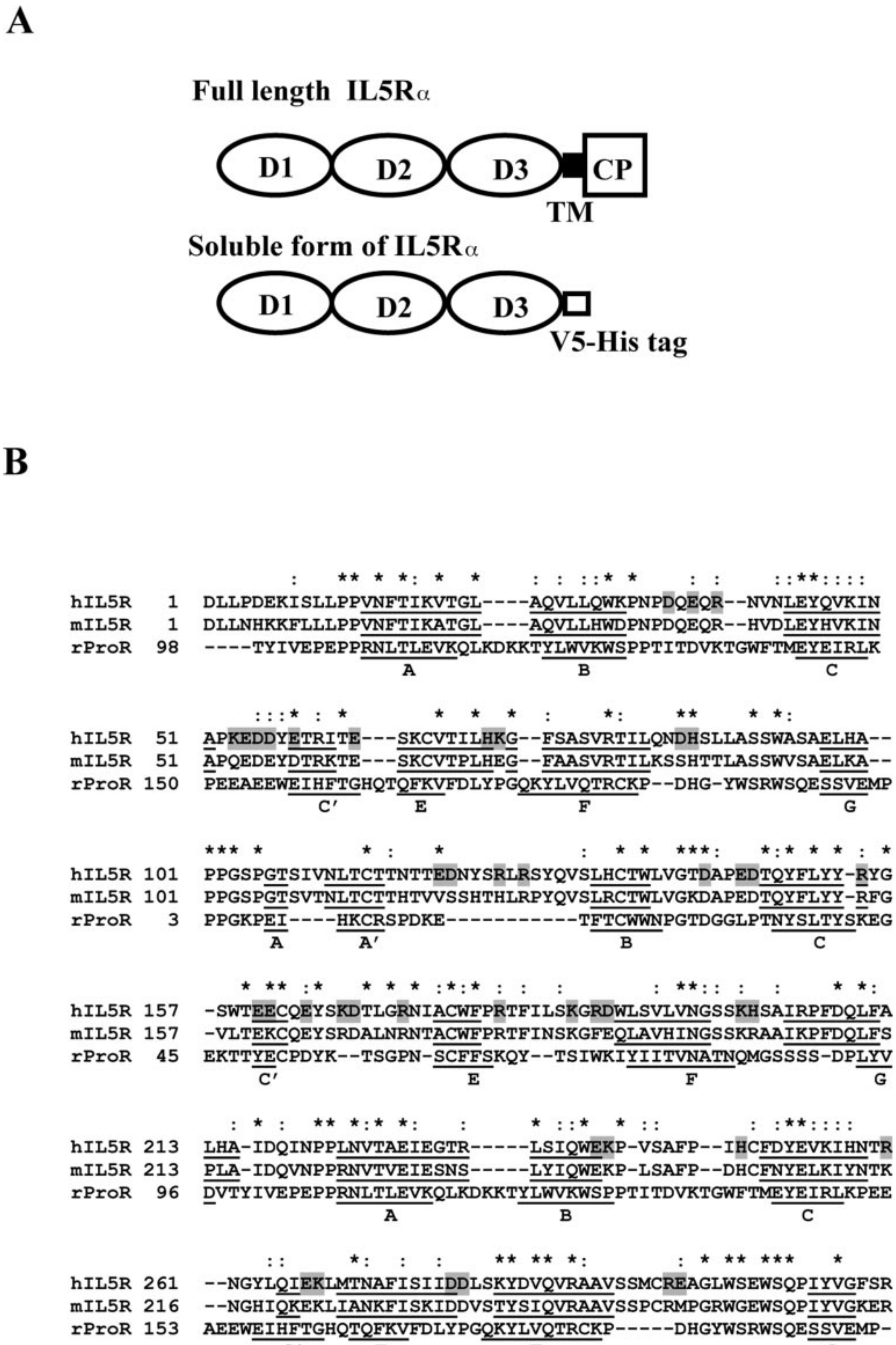

FIG. 1. **Extracellular domain construct of IL5Rα used in biosensor analysis of mutational variants.** *A*, comparison of soluble form of IL5Rα (*lower*) used in antibody-capture binding assay with full-length IL5Rα (*upper*) composed of an extracellular region (*D1*, *D2*, and *D3*), a transmembrane (*TM*) region and a cytoplasmic (*CP*) region. The soluble form of IL5Rα (sIL5Rα) corresponds to the extracellular region. V5-His tag was fused at the C-terminal region of D3 that normally adjoins the TM region. *B*, sequence alignment of extracellular regions of human and mouse IL5Rα, and rat prolactin receptor. Identical amino acid residues are marked by *asterisks*, and similar amino acid residues are marked by the ":" symbol. Multiple sequence alignments were performed by using PSI-BLAST (27) and ClustalW 1.60 (43), both of which provided similar results. Alignments were further adjusted manually (see "Experimental Procedures"). Groups of similar amino acid residues were categorized according to ClustalW 1.60. *Underlines* in the prolactin receptor sequence show the β-strand regions determined by its crystal structure (26). An alignment of the human growth hormone and human IL5Rα was initially used to design the position of mutagenesis, whereas crystal structure of rat prolactin receptor was used for homology modeling. The β-strand regions estimated from human growth hormone and rat prolactin receptor were essentially the same, except for the β-strand G in D2 domain. *Shaded* are the residues that were substituted by alanine in this study.

Individual k_{on}, k_{off}, and K_d values were obtained from at least three separate experiments.

Homology Modeling—The D1 and D2D3 domains of human IL5Rα were modeled separately using the crystal structure of the D2 and D1D2 domains of the rat prolactin receptor (26), which were identified with a low *E* value by PSI (Position-specific Iterative) BLAST search

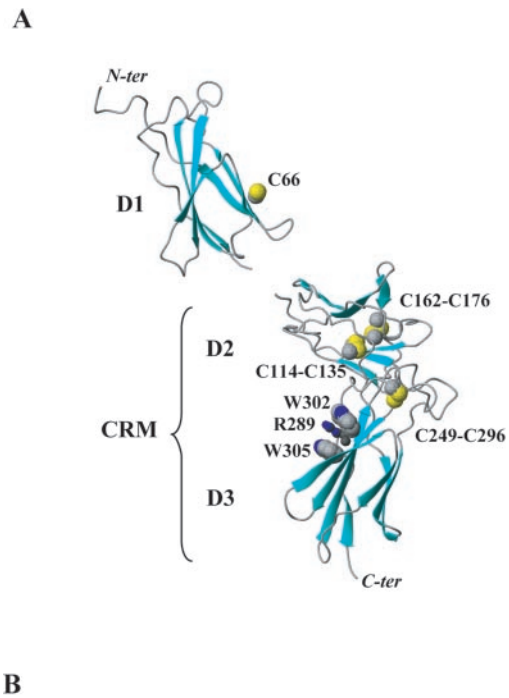

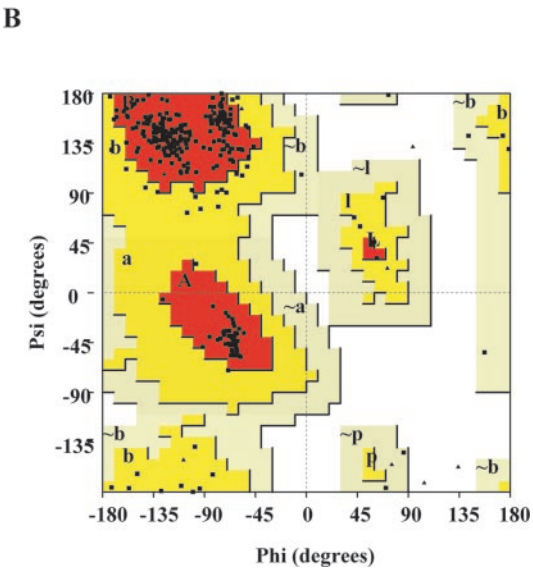

FIG. 2. **Basic features and Ramachandran plot of modeled structure of sIL5Rα.** A, homology model of the tertiary structure of the extracellular region of IL5Rα. Loops are represented as *coils* and β-strands as *ribbons*. In this structure, each fibronectin type III domain of IL5Rα is termed D1, D2, and D3 from the N to the C termini, which are labeled *N-ter* and *C-ter*, respectively. D2 and D3 domains have sequence homology with the classic cytokine recognition motif (CRM). Seven cysteine residues are shown as CPK (Corey Pauling Kultin) models and labeled by residue type and number. One disulfide bond (Cys^{114}-Cys^{135}) links the neighboring strands A and B and another disulfide bond (Cys^{162}-Cys^{176}) links strands D and E. In this modeled structure, a disulfide bond between Cys^{249} and Cys^{296} in D3 domain was introduced (see "Experimental Procedures"). The guanidinium group of Arg^{290} was intercalated between the two indole rings from the WS*X*WS motif in D3 domain. The tryptophan residues are shown as CPK models, and the arginine residue is shown as a *ball-and-stick* model. All the molecular graphic figures in this article were prepared with the program MOLMOL (42). *B*, the Ramachandran plot analysis by PROCHECK (30) showed that 85.5% of non-glycine and non-proline residues fell into the most favored regions, 12.4% into the additional allowed regions, 2.1% into the generously allowed regions, and no non-glycine residues in disallowed regions.

(27). The Cartesian coordinate of chain B in Protein Data Bank ID 1F6F, which corresponds to the high affinity receptor of rat prolactin receptor, was used as a template. The sequence alignments obtained with PSI BLAST search were manually modified by considering the

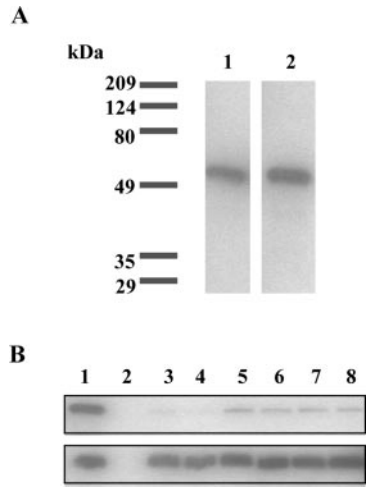

FIG. 3. **Western blotting of sIL5Rα variants.** *A*, Western blotting of secreted wild type sIL5Rα. *Lane 1* shows the band stained by anti-human IL5Rα polyclonal antibody; *lane 2*, the band stained by anti-histidine tag polyclonal antibody. *B*, Western blotting of the supernatants (*upper*) and precipitates (*lower*) of non-secretion variants by anti-histidine tag polyclonal antibody: *lane 1*, positive control (wild type IL5Rα); *lane 2*, negative control (empty vector transfection); *lane 3*, H71A; *lane 4*, K167A/D168A; *lane 5*, R172A; *lane 6*, D189A; *lane 7*, R260A; and *lane 8*, D279A/D280A.

conserved residues and the alternating pattern of hydrophobic residues in the class I cytokine superfamily (18). The final sequence alignments showed 21% identity and 42% similarity for D1 domain and 25% identity and 43% similarity for D2D3 domains of IL5Rα (Fig. 1*B*). These sequence alignments were used to build tertiary structures of D1 and D2D3 domains by means of a comparative homology modeling method. An ensemble of 50 structures was generated by the program MODELLER (28). In the initial modeling process, we noticed that sulfhydryl groups of Cys^{249} and Cys^{296} residues in D3 domain are close in three-dimensional space, supporting the prediction of the disulfide bridge between them (29). Therefore, the disulfide bond between Cys^{249} and Cys^{296} was added as a restraint condition. Basic steric principles such as close contacts or violation of stereochemistry were examined using the PROCHECK program (30), and the three-dimensional profiles of the models were examined using the program ProsaII (31). Based on these quality checks, the best modeled structures were chosen. To interpret the result of mutational analysis, IL5 (crystal structure (13)) and IL5Rα D2D3 domain (modeled structure) were superimposed on the crystal structure of the placental lactogen complex with prolactin receptor (26). Finally, the structure of D1 domain of IL5Rα was manually aligned to the structure of D2D3 domain, because there is no information on the relative orientation between D1 and D2 domains.

The final model (Fig. 2*A*) exhibited good stereochemistry and showed that no residues fell into disallowed regions of phi-psi space (a Ramachandran plot is shown in Fig. 2*B*). The accuracy of the modeled structures was also assessed by using the ProsaII program, which is based on Eisenberg's three-dimensional profile method (32). The combined *Z*-scores (ProsaII terminology) for D1 and D2D3 domains were −4.12 and −4.88, respectively, which are low enough to consider the predicted structures reliable. The *Z*-scores of template structures were −4.96 and −6.98, respectively. The higher *Z*-score of D2D3 domains than that of the template was attributed to the long loop insertion between strands A and B in D2 domain, judging from the ProsaII energy plot (data not shown). Modeled structures of D1 and D2D3 domains appear reasonable in several important ways. First, the modeled structures had the basic features, such as disulfide bonds in D2 domain and the spatial alignments of conserved tryptophan and arginine residues in D3 domain, which are commonly seen in the structures of class I cytokine receptors (Fig. 2*A*). It may be noted that three of four *N*-glycosylation sites in human IL5Rα were conserved with rat prolactin receptors. The modeled structures showed that the amide groups of Asn^{15}, Asn^{111}, Asn^{196}, and Asn^{224} in the estimated *N*-glycosylation sites were exposed to solvent and seem to have enough space for post-translational modification by bulky carbohydrate moieties.

RESULTS

Expression and Antibody Capture of sIL5Rα Mutational Variants—We systematically replaced the charged amino acid residues (aspartic acid, glutamic acid, arginine, lysine, and histidine) of human sIL5Rα singly or doubly to alanine. To reduce the number of the mutants that had to be made, we chose the residues in the predicted loop regions, which are generally employed to bind a ligand in class I cytokine receptors (Fig. 1*B*). Almost all of the mutational variants made in this study were expressed in *Drosophila* S2 cells and secreted into the cell culture in roughly equal amounts (30–40 nM), as judged by Western blot analysis (Fig. 3*A*). Expression of secreted proteins was taken as an indicator that these molecules were stably folded. Six variants failed to secrete into the culture media (Fig. 3*B*). Alanine substitutions in these variants (H71A, K167A/D168A, R172A, D189A, R260A, and D279A/D280A) might have caused unstable structure or reduction of solubility. It cannot be ruled out from our current data that these residues could be involved in ligand binding. All of the non-secreted variants were found to be remote from the deduced epitope for IL5 binding (see "Discussion"). Five of these variants are for residues in D2 (K167A/D168A, R172A, and D189A) or in D3 (R260A and D279A/D280A). These residues may well stabilize the structure through internal interactions.

We examined the ability of anti-V5 tag antibody, α16, and 2B6R to capture wild type sIL5Rα. Cell-free culture supernatant containing sIL5Rα was injected onto all the flow cells. The three antibodies could capture sIL5Rα selectively, while few nonspecific components were bound to the positive control surface. The optimal regeneration condition, for removing sIL5Rα from anti-V5 tag antibody and α16, was 10 mM glycine-HCl, pH 1.5. This condition was effective in both removing all sIL5Rα and preserving the capturing capacity of the antibodies (less than 1% loss of capacity per cycle). However, the conditions we tested for 2B6R caused a more than 5% loss of the capturing capacity after each cycle of capture and regeneration, and therefore we omitted use of 2B6R in further experiments.

Next, we compared the capture of the secreted sIL5Rα variants using anti-V5 tag antibody and α16. Anti-V5 tag antibody captured all the variants as much as wild type sIL5Rα. As expected, these alanine substitutions did not affect the interaction between C-terminal V5 tag and anti-V5 tag antibody. On the other hand, α16 could not capture three variants, D142A, E145A/D146A, and K200A/H201A. Fig. 4*A* shows real-time sensorgrams during the capturing process when wild type sIL5Rα and the variants were injected onto the α16 immobilized surface. Alanine substitutions of Glu^{145} and Asp^{146} completely impaired the interaction with α16, indicating that these two residues are crucial for α16 binding. Interestingly, Glu^{145} and Asp^{146} residues are located at the top of D2 domain and are surrounded by Asp^{142}, Lys^{200}, and His^{201} (Fig. 4*B*), whose alanine substitution diminished α16 capturing.

IL5 Binding Activity of sIL5Rα Variants—The kinetics of interaction between human IL5 and sIL5Rα was measured by using a sandwich surface plasmon resonance biosensor method (Fig. 5*A* (14)). Although IL5 is a homodimeric protein, it has been shown that the stoichiometry of IL5·IL5Rα interaction is 1:1 (10, 12), and a Langmuir 1:1 binding model has been used for global fitting analysis of IL5·IL5Rα interaction (33). In this article, we first measured the association rates at flow rates of a range of 10 to 80 μl/min to examine the mass transfer effect (Fig. 5*B*). Because the flow rates of 40 and 80 μl/min did not alter the measured association rates, the kinetic assays were performed at a flow rate of 50 μl/min. Even at such a high flow rate, however, we subsequently observed a slight dependence of kinetic parameters on the amount of captured proteins, and we

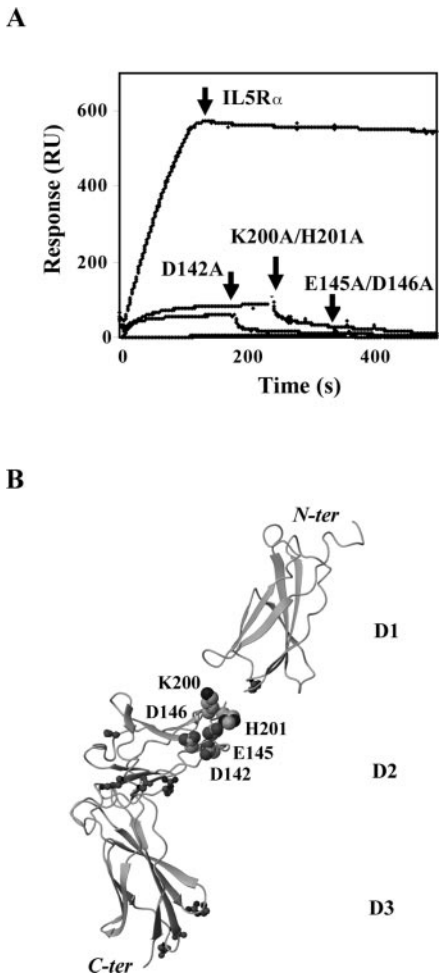

FIG. 4. **Epitope analysis and mapping for a non-neutralizing anti human IL5Rα antibody α16.** *A*, Biacore-derived real-time sensorgrams of the interactions of wild type IL5Rα and receptor α variants, which impaired the high affinity interaction with α16. Receptor samples were injected onto the immobilized α16 surface at zero time, and *arrows* shows the time when the injections reverted to buffer alone. *B*, mapping of the α16 epitope on the modeled structures of IL5Rα. Residues that impaired, through alanine substitution, the high affinity interaction with α16 are shown as CPK models and labeled by residue type and number. Residues that caused non-secretion through alanine substitutions (Table II) are shown as *ball-and-stick* models.

concluded that the binding of IL5 can be compromised by mass transfer effect. In fact, the fitting was improved by using a model of 1:1 binding with mass transfer (Table I). Hence, we used the latter binding model for further data analysis. The ratio of the R_{max} value *versus* the captured IL5Rα is ~3:7, whereas the estimated molecular weight ratio of IL5 *versus* sIL5Rα is ~3:5 (Table I). Mutational variants of IL5Rα had a similar ratio. This confirms that 1:1 binding stoichiometry is occurring in all cases. Fig. 5*C* shows the full sensorgrams for wild type sIL5Rα. After repetitive injections of the culture media, the same level of capturing was observed for each cycle. Various concentrations of IL5 were then injected. The rate constants (k_{on} and k_{off}) were calculated by fitting the association phase (Fig. 5*C*, *c* and *d*) and dissociation phase (*d* and *e*) to a model of 1:1 Langmuir binding with mass transfer. Fig. 5*D* shows the sensorgrams and fitting curves for association and dissociation of IL5 analyte. The fitting parameters as well as kinetic parameters obtained are summarized in Table I. The rate constants for wild type sIL5Rα were similar to the values measured previously for purified IL5 and sIL5Rα (11, 12, 33).

The above kinetic interaction assay was applied to alanine-scanning mutational variants of sIL5Rα. For comparison, rel-

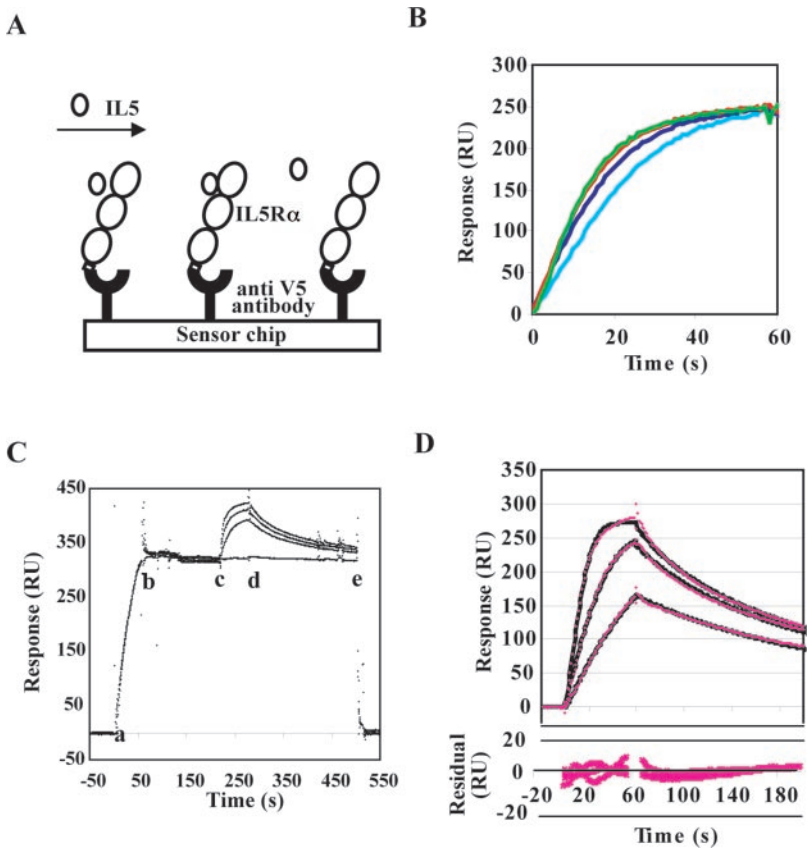

FIG. 5. **Biosensor binding analysis of sIL5Rα.** *A*, anti-V5 tag monoclonal antibody was covalently immobilized to the dextran matrix on a sensor chip gold surface. sIL5Rα was captured on the surface via tight interaction of V5 tag and the antibody, providing the similar configuration to cell surface receptors. IL5 was then injected to the sIL5Rα-captured surface, and its kinetic interaction was examined. *B*, the effect of flow rate. The association rates were measured at flow rates of 10, 20, 40, or 80 μl/min (*cyan*, *blue*, *green*, or *red*, respectively). *C*, overlay of real-time sensorgrams shows sequential injections of cell-free media containing sIL5Rα (*a*), injection of running buffer (*b*), injections of 0, 12.5, 25, and 50 nM of IL5 (*c*), injection of running buffer alone (*d*), and injections of the regeneration buffer (*e*). *D*, global fitting of wild type IL5Rα. Various concentrations of IL5 (0, 12.5, 25, and 50 nM) were injected. The rate constants were calculated by fitting the association phase and dissociation phase to a model for 1:1 Langmuir binding with mass transfer. Residuals are shown in the *lower panel* of *D*. *Magenta dots* show experimental sensorgrams, and *black lines* show calculated sensorgrams.

TABLE I
Global fitting analysis of kinetic interaction between IL5 and sIL5Rα

Fitting model	$k_{on} \times 10^{-6}$	$k_{off} \times 10^{3}$	$K_d \times 10^{9}$	R_{max} [a]	Chi^2 [a]
	$M^{-1}s^{-1}$	s^{-1}	M	RU	
1:1	2.4 ± 0.7	7.2 ± 1.6	3.1 ± 0.5	273	29
1:1 with mass transfer	4.2 ± 0.4	11 ± 1.7	2.8 ± 0.3	277	5.1

[a] R_{max} and Chi^2 values were calculated from an experiment, in which captured IL5Rα was 680 RU.

ative values for k_{on}, k_{off}, and K_d determined using anti-V5 tag antibody capturing are listed in Table II. Six of the mutations resulted in a marked (more than 3-fold) reduction in the binding affinity, that is, an increase in the K_d value. This can be seen visually in Fig. 6 (*A* and *B*). These activity-suppressing mutations were found to occur in each domain of IL5Rα, namely, in D1 (D55A, D56A, and E58A), D2 (K186A and R188A), and D3 domains (R297A). A slight (1.5- to 3-fold) increase in the K_d value was also found for other D1 (E63A and K53A/E54A) and D3 (E239A/K240A) residues. For all the mutants, the kinetic parameters were also determined using α16 capturing, except for the α16 epitope mutants. The K_d values from the α16-capturing method were similar to those from the anti-V5 tag antibody method (data not shown).

Among the affinity-decreasing mutations mentioned above, only four mutations, D55A, D56A, E58A, and R188A, were found to decrease the k_{on} (Table II). These variants also showed an increase in the k_{off}, and with resulting drastic decrease in binding affinity. Remarkably, the mutations D55A and R188A caused slower association rates and faster dissociation rates each by a factor of about 10, leading to overall decreases in the binding affinities of 160- and 60-fold, respectively. Global fitting analyses of D55A and R188A are shown in Fig. 6 (*C* and *D*) as examples. In contrast, such mutations as K53A/E54A, E63A, K186A, E239A/K240A, and R297A were found to increase the k_{off} without affecting the k_{on}. Of these variants, K186A and R297A caused marked effects, 5- to 8-fold faster dissociation rate. None of the mutants had effects only on the k_{on}. In the previous experiments, similar dominance of the dissociation rate constant was observed in kinetic analysis of IL5 mutants, in which loss of the binding affinity was mainly caused by an increase in the dissociation rate constant (14, 34). This phenomenon might reflect mechanistic features of the IL5·IL5Rα interaction (see "Discussion").

We also found that several mutations caused an increase in the binding affinity. On the whole, this change was much smaller (1.5- to 2-fold decrease in the K_d) than that of affinity-decreasing mutations. As shown in Table II, these decreased K_d values were attributed to increases in the k_{on} (D85A/H86A, E145A/D146A, and K200A/H201A) or decreases in the k_{off} (H248A and E298A). It should be noted that some of the residues of affinity-increasing mutations, such as E145A/D146A and K200A/H201A, are in the putative binding epitope for α16 antibody. One may speculate that reducing charge in this latter region increases the IL5 binding affinity by conformational changes within IL5Rα, because the epitope for α16 (non-neutralizing antibody) is remote from the IL5 binding sites in our modeled structure (Fig. 4*B*).

Although charged amino acid residues are usually exposed to solvent and hence unlikely to reside in the hydrophobic core of the protein, we examined the possibility that they could have an impact on structural integrity by calculating the solvent-accessible surface area. As shown in Table II, all the residues that were sensitive to alanine substitutions were found to be

TABLE II
Relative rate constants and dissociation constants of IL5Rα mutants

	Relative $1/k_{on}$	Relative k_{off}	Relative K_d	SA[a]	α16 capture[b]
					%
IL5Rα	1	1	1		100
D1 mutants					
D35A/E37A	0.99	1.2	1.3	40	109
R39A	0.97	1.2	1.2	60	97
K53A/E54A	0.97	1.8	1.7	46	100
D55A	11	14	156	55	96
D56A	1.6	6.8	17	34	117
E58A	1.7	1.6	3.0	17	99
E63A	1.0	2.2	2.2	43	96
H71A			Not secreted	49	
K72A	0.85	1.5	1.3	35	44
D85A/H86A	0.57	1.1	0.60	34	88
D2 mutants					
E120A/D121A	1.2	1.2	1.3	12	117
R125A/R127A	0.70	1.7	1.2	68	106
D142A	0.90	1.1	1.0	19	3.4
E145A/D146A	0.51	1.2	0.62	36	1.6
R154A	0.69	1.3	0.92	14	59
E160A/E161A	0.82	1.1	0.86	23	63
E164A	0.89	1.1	0.97	5.4	84
K167A/D168A			Not secreted	25	
R172A			Not secreted	56	
R180A	0.79	1.7	1.3	35	72
K186A	0.70	5.4	3.7	32	114
R188A	6.2	8.9	58	58	106
D189A			Not secreted	12	
K200A/H201	0.75	0.98	0.75	52	4.8
D3 mutants					
E239A/K240A	0.67	2.5	1.6	27	101
H248A	0.99	0.67	0.64	3.3	77
R260A			Not secreted	34	
E267A/K268A	0.87	0.92	0.78	21	93
D279A/D280A			Not secreted	30	
R297A	1.0	8.0	7.6	40	80
E298A	1.2	0.56	0.52	36	85

[a] Percent solvent-accessible surface area (%SA) was calculated with the CalcSurface routine in the program MOLMOL (42).
[b] Percent α16 capture was calculated by dividing amounts of α16-captured proteins by those V5-captured proteins, and then by dividing the resulting values of mutants by that of wild type IL5Rα.

highly solvent-accessible (>15%), with one exception of H248A (3.3%). Alanine substitution of histidine at position 248 might decrease the k_{off} by stabilizing the local structure of the complex. Furthermore, it would be possible to estimate the structural integrity of the variants judging from the amount of α16 capturing, because α16 is a conformation-sensitive antibody (data not shown). These affinity-sensitive variants were captured by α16 as much as wild type IL5Rα (Table II), indicative of the integrity of structure. Thus, loss of ligand binding activity for the key mutations reported in the present study can be interpreted as due largely to diminishing the inter-molecular interaction required for ligand recognition and not to destabilization of receptor conformation. This is consistent with the secretability of these variants.

DISCUSSION

Sandwich Binding Assay—The purpose of this study was to elucidate the molecular recognition mechanism of the IL5·IL5Rα system using kinetic interaction analysis of alanine-scanning mutational variants of human sIL5Rα. To analyze kinetic interactions of a large number of proteins, we established a sandwich surface plasmon resonance biosensor method. In this method, receptor α protein is selectively captured by its antibody from heterogeneous cell culture media, providing a homogeneous surface for the subsequent quantitative ligand binding assay. Early success of this methodology was achieved by using IL5 and its non-neutralizing monoclonal antibody (14). In the present study, we introduced a new sandwich binding assay using C-terminal V5 tag and anti-V5 tag antibody. This configuration appears more advantageous than the previous sandwich assay, because the captured receptor can be oriented analogously to receptors on a cell surface and mutations in receptor sequences do not affect the affinity capture process. Our results demonstrated that anti-V5 tag antibody captured all the mutational variants. In contrast, α16 failed to capture some variants when alanine substitution occurred in the epitope of the antibody (Fig. 4). Similar strategies have been reported for transforming growth factor-β and its receptor using a coiled-coil capture system where the receptor fused with C-terminal "E coil" tag is captured by "K coil' immobilized onto the sensor chip (35). We investigated the kinetic interaction of 25 mutational variants of sIL5Rα using a V5 tag and anti-V5 tag antibody system and could demonstrate an example of medium throughput kinetic assay of receptor mutagenesis without necessity of receptor purifications. This medium throughput sandwich binding assay for kinetic interaction is applicable to other ligand-receptor systems.

Binding Topology of IL5Rα—The IL5Rα alanine-scanning mutagenesis was focused on charged amino acid residues. This is because the receptor-binding residues in human IL5 appear to be mostly charged amino acids such as arginine and glutamic acid (reviewed in ref. 36), and these amino acids can be surmised to interact with oppositely charged amino acid residues of the receptor through salt bridge or hydrogen bond interactions. The important epitope residues identified in the present study, Asp^{55}, Asp^{56}, Glu^{58}, Lys^{186}, Arg^{188}, and Arg^{297} are the most likely candidates to be involved in direct interaction with IL5 ligand. The residues of minor importance, namely, Glu^{63}, either Lys^{53} or Glu^{54} and either Glu^{239} or Lys^{240}

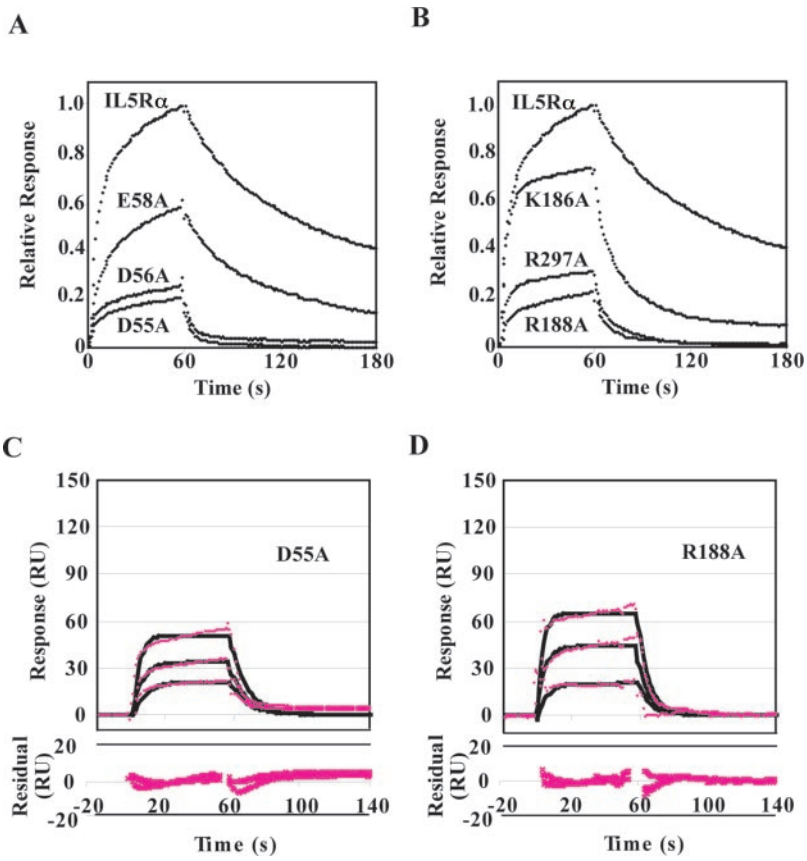

FIG. 6. **Mutations that diminished the high affinity interaction of IL5Rα with IL5.** Binding curves of (*A*) the D1 mutants and (*B*) the D2D3 mutants, which markedly decreased the binding affinity. Each sensorgram shows the association (0–60 s) and dissociation (60–180 s) of IL5 (50 nM) to sIL5Rα or the mutational variants captured by anti-V5 tag antibody. For comparison, sensorgrams were normalized depending on the amount of captured protein. Various concentrations of IL5 (0, 50, 100, and 250 nM) were injected to captured D55A variant (*C*) or R188A variant (*D*). The interaction curves were globally fit using Langmuir 1:1 binding with mass transfer. Residuals are shown in the *lower panels* in *C* and *D*. *Magenta dots* show experimental sensorgrams, and *black lines* show calculated sensorgrams.

may be involved more indirectly. Interestingly, these amino acid residues are conserved in human and mouse, except for Lys^{53} and Arg^{188}, which are glutamine and phenylalanine residues in mouse, respectively (Fig. 1*B*). IL5Rα genes have not been cloned from the other species so far, but our data suggest that these conserved residues might be key residues for IL5 recognition of other IL5 species.

The current mutagenesis data demonstrated a binding topology in which all three extracellular domains of IL5Rα are involved in the direct interaction with IL5. Previously, chimeric analysis had demonstrated the importance of D1D2 domains of human IL5Rα, based on site-directed mutagenesis showing that Asp^{55}, Asp^{56}, Tyr^{57}, Glu^{58}, and Arg^{188} are crucial for the high affinity interaction with human IL5 (21). The current data fit well with the fact that it is the D2D3 domains of IL5Rα that have sequence homology with the minimum cytokine-recognizing unit (CRM). Up to now, the role of D3 domain in IL5Rα has been less understood. In the present article, we defined Arg^{297}, and either Glu^{239} or Lys^{240}, as involved in IL5 binding. This finding demonstrates that the D3 domain is also important for ligand binding. With regard to D1D2 mutants, a rough correlation was observed between our data and those obtained previously (21), with the exception of K53A/E54A, E63A, and K186A, which we have newly identified in the current study. In contrast to other class I cytokine receptors, the CRM of IL5Rα (D2D3) is not sufficient for the full binding activity, and the additional FnIII domain (D1) is instead used to form an extended cytokine recognition interface.

The finding that the D3 domain is involved in the direct interaction is consistent with many aspects of previous reports. First, Czabotar *et al.* have recently reported that the D3 domain is involved in cell proliferation activity of IL5Rα, which was measured by the extent of thymidine incorporation into cells (37). Their mutational analysis further showed the importance of the F-G loop, in which Arg^{297} is located. The purpose of this study was to investigate the mutational effects on binding interaction, but our data are consistent with the physiological data. Second, Devos *et al.* (29) have reported that serine substitutions of Cys^{249} and Cys^{296} residues, which are close to Arg^{297} in the D3 domain, resulted in complete loss of IL5 binding activity. These cysteine residues appear to be linked through a disulfide bridge, which likely stabilizes a structure that presents Arg^{297} in the correct spatial configuration. Third, Rajotte *et al.* (38) have demonstrated that Arg^{280} of GM-CSF receptor α chain, which corresponds to Arg^{297} of IL5Rα, plays a crucial role for ligand recognition. They have proposed that the side chain of Arg^{280} possibly interacts with the side chain of Asp^{112} of the ligand, which corresponds to Glu^{110} of IL5. It is noteworthy that there is an arginine residue at the position 259 in IL3 receptor α chain, which is assigned to Arg^{297} of IL5Rα and Arg^{280} of GM-CSF receptor α chain in our sequence alignment (data not shown). Out of the residues that diminished the binding affinity in our current experiment, Arg^{297} is the only conserved residue among these three receptors. Because α receptors for IL3, IL5, and GM-CSF share the signal-transducing receptor βc, these arginine residues could be important for βc recruitment as well as ligand binding.

Charge Distribution for IL5 Recognition—The important IL5-binding residues were mapped on the deduced ternary structure of human IL5Rα, revealing that the binding epitope comprises two discontinuous regions (Fig. 7). One is a negatively charged patch formed by Asp^{55}, Asp^{56}, and Glu^{58} in D1 domain, and the other is a positively charged patch formed by Lys^{186}, Arg^{188}, and Arg^{297} at the interface of D2 and D3 domains. Although Arg^{297} residue is distant from Lys^{186} and Arg^{188} in the primary sequence, these three residues are in close spatial proximity in the modeled structure. Because the D2D3 domains correspond to CRM, it is interesting to look at the equivalent positions of Lys^{186}, Arg^{188}, and Arg^{297} in the CRM of prolactin receptor (the template of homology modeling;

Fig. 1*B*), which are Ser[70], Trp[72], and His[188], respectively. Interestingly, these residues are all in the binding surface of the complex structure (26). In particular, side chains of Trp[72] and His[188] form hydrogen bonding interactions with the prolactin ligand. This observation strongly indicates that D2D3 domains of IL5Rα function as a unit, like other CRMs of the class I cytokine receptor superfamily. Taken together, IL5 can be viewed to recruit receptor α by a D1 domain and a D2D3 tandem domain, which are structurally distinguishable units of the receptor.

The dominant importance of the opposing negative and positive charge distribution in IL5Rα correlates with previously elucidated IL5 mutations showing that Arg[91] (and the overall positive charge balance of the CD turn region), and Glu[110] are two main IL5 charged sites for IL5Rα recognition (15–17). Although the detailed structural description of the IL5·IL5Rα interaction must await high resolution structure determination of the IL5·IL5Rα complex by x-ray crystallography or NMR spectroscopy, it is tempting to speculate that the side chains of Arg[91] and Glu[110] of IL5 might come into contact with the negatively charged patch in D1 and the positively charged patch in D2D3, respectively (Fig. 7). It has been found that the known functionally important CD turn sequence [88]EERRR[92] in IL5 can be replaced by [88]SLRGG[92] and that the positive charge in this turn is thought to be the key factor promoting IL5Rα recruitment (17). Among other things, we can speculate that the positive charge balance in the CD turn region interacts directly with the negatively charged patch of the D1 domain. Of note, it should not be ignored that alanine substitution of Glu[298], which is adjacent to Arg[297], increased the binding affinity due to a 2-fold decrease in the k_{off} (Table II). This decreased dissociation rate may reflect the reduction of electrostatic repulsion near the interface of Glu[298], possibly against Glu[110] of IL5. From these observations, we hypothesize that a pair of charge complementary regions may play an important role in specific interaction between IL5 and IL5Rα.

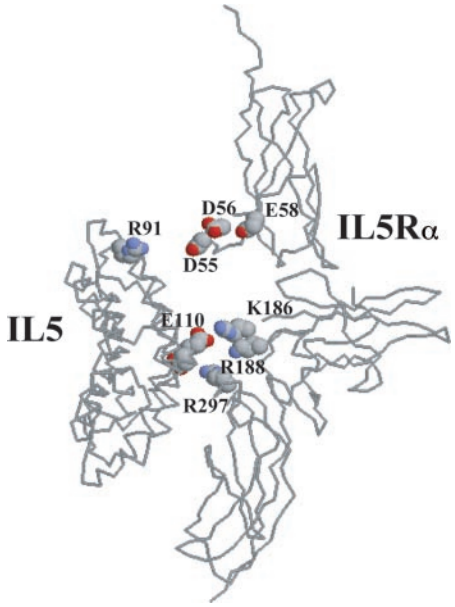

FIG. 7. **Hypothetical structure of the IL5 complex with IL5Rα.** Both IL5 (*R91* and *E110*) and IL5Rα (*D55*, *D56*, *E58*, *K186*, *R188*, and *R297*) epitope residues are expressed in the CPK model.

Ligand Recognition Mechanism of IL5Rα—Kinetic analysis of the IL5·IL5Rα interaction demonstrated that Asp[55] and Arg[188] had the biggest effect on the fast association of the interaction, with more minor contributions from Asp[56] and Glu[58]. These residues are located in D1 and D2 domains, as shown in Fig. 8*A*. Association pathway of a protein-protein interaction can be viewed as a stepwise process, in which the proteins initially encounter in nonspecific fashion, followed by rearrangements that evolve the final complex. The reduction in the k_{on} can correlate with the reduction in electrostatic steering effect during the initial encounter step. In the case of IL5·IL5Rα interaction, however, the k_{on} is 3×10^6 M^{-1} s^{-1}, which is comparable to 2×10^6 M^{-1} s^{-1}, the value predicted by the Brownian dynamics simulation without any assumptions of steering forces (39). So what causes the reduction in the k_{on}? Previously, kinetic and structure studies of the anti-lysozyme antibody D1.3 have indicated that local conformational adaptation is responsible for the association rate (40). Furthermore, statistical thermodynamic analysis of the same antibody has shown that the binding effects can propagate to a subset of residues at distal sites when the binding sites include the region with conformational fluctuations (41). The slower association rate upon mutation in D1D2 domains might be explained by the ineffective propagation of preferential conformation, which is required during the rearrangement step of association. This explanation seems to be in good agreement with the thermodynamics analysis data that considerable

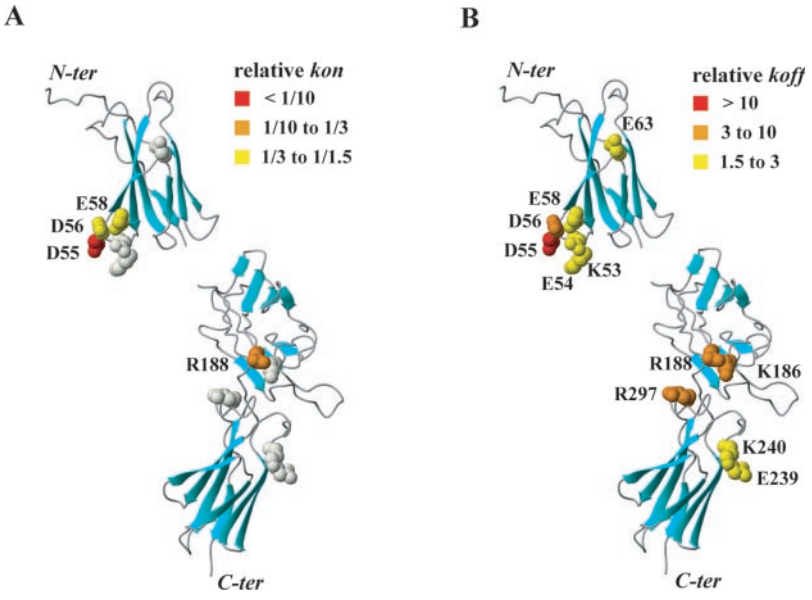

FIG. 8. **Maps of IL5 binding residues on the modeled structure of sIL5Rα.** Residues that decreased, through alanine substitution, the binding affinity by a factor of more than 1.5 are shown as CPK models. *A*, residues responsible for first association rate are *colored according to the decrease in the rate constant*, k_{on}. *B*, residues responsible for slow dissociation rate are colored according to the increase in the rate constant, k_{off}.

structural rearrangement is coupled to the IL5·IL5Rα interaction (12). Taking account of the impact of the D1D2 residues on the fast association, this structural rearrangement possibly takes place in D1D2 regions. The conformational change may allow the D3 domain to be involved in the interaction and induce the transition state of IL5Rα for βc recruitment. The effects on the k_{off} were identified in the residues from the whole domains of IL5Rα (Fig. 8*B*). This observation again confirms the involvement of D1, D2, and D3 domains in the final complex, because the dissociation rate of a protein-protein interaction can be attributed simply to destabilizing the final mature complex.

In summary, the present study reveals the essential role of charged residues in interaction of IL5Rα with IL5. The main determinants, Asp^{55}, Asp^{56}, Glu^{58}, Lys^{186}, Arg^{188}, and Arg^{297} are distributed over the D1, D2, and D3 domains of IL5Rα. The IL5 binding epitope residues assemble in structurally discontinuous sub-regions, which are constituted by a negatively charged patch in D1 domain and a positively charged patch at the D2D3 interface. These results suggest that the IL5·IL5Rα system adopts a unique binding topology, in which the cytokine is recognized by a D1 domain and a D2D3 tandem domain (CRM) to form an extended cytokine recognition interface. Revealing the key recognition elements of IL5Rα, and its charge complementarity of IL5 could help drive the design of new compounds for therapeutic treatment against IL5-related allergic inflammatory diseases.

Acknowledgment—We thank Dr. Jan Tavernier (University of Ghent, Ghent, Belgium) for the gift of α16 monoclonal antibody.

REFERENCES

1. Karlen, S., De Boer, M. L., Lipscombe, R. J., Lutz, W., Mordinov, V. A., and Sanderson, C. J. (1998) *Int. Rev. Immunol.* **16,** 227–247
2. Plaetinck, G., Van der Heyden, J., Tavernier, J., Fache, I., Tuypens, T., Fischk_{off}, S., Fiers, W., and Devos, R. (1990) *J. Exp. Med.* **172,** 683–691
3. Tavernier, J., Devos, R., Cornelis, S., Tuypens, T., Van der Heyden, J., Fiers, W., and Plaetinck, G. (1991) *Cell* **66,** 1175–1184
4. Lopez, A. F., Elliott, M. J., Woodcock, J., and Vadas, M. A. (1992) *Immunol. Today* **13,** 495–500
5. Goodall, G. J., Bagley, C. J., Vadas, M. A., and Lopez, A. F. (1993) *Growth Factors* **8,** 87–97
6. Mckinnon, M., Banks, M., Solari, R., and Robertson, G. (1999) in *Interleukin-5: From Molecule to Drug Target for Asthma* (Sanderson, C., ed) pp. 299–320, Marcel Dekker. Inc., New York
7. Foster, P. S., Hogan, S. P., Yang, M., Mattes, J., Young, I. G., Matthaei, K. I., Kumar, R. K., Mahalingam, S., and Webb, D. C. (2002) *Trends Mol. Med.* **8,** 162–167
8. Murata, Y., Takaki, S., Migita, M., Kikuchi, Y., Tominaga, A., and Takatsu, K. (1992) *J. Exp. Med.* **175,** 341–351
9. Tavernier, J., Tuypens, T., Plaetink, G., Verhee, A., Fiers, W., and Devos, R. (1992) *Proc. Natl. Acad. Sci. U. S. A.* **89,** 7041–7045
10. Devos, R., Guisez, Y., Cornelis, S., Verhee, A., Van der Heyden, J., Manneberg, M., Lahm, H. W., Fiers, W., Tavernier, J., and Plaetinck, G. (1993) *J. Biol. Chem.* **268,** 6581–6587
11. Morton, T. A., Bennett, D. B., Appelbaum, E. R., Cusimano, D. M., Johanson, K. O., Matico, R. E., Young, P. R., Doyle, M., and Chaiken, I. M. (1994) *J. Mol. Recognit.* **7,** 47–55
12. Johanson, K., Appelbaum, E., Doyle, M., Hensley, P., Zhao, B, Abdel-Meguid, S. S., Young P., Cook, R., Carr, S., Matico, R., Cusimano, D., Dul, E., Angelichio, M., Brooks, I., Winborne, E., McDonnell, P., Morton, T., Bennett, D., Sokoloski, T., McNulty, D., Rosenberg, M., and Chaiken, I. (1995) *J. Biol. Chem.* **270,** 9459–9471
13. Milburn, M. V., Hassell, A. M., Lambert, M. H., Jordan, S. R., Proudfoot, A. E., Graber, P., and Wells, T. N. (1993) *Nature* **363,** 172–176
14. Morton, T., Li, J., Cook, R., and Chaiken, I. (1995) *Proc. Natl. Acad. Sci. U. S. A.* **92,** 10879–10883
15. Graber, P., Proudfoot, A. E., Talabot, F., Bernard, A., McKinnon, M., Banks, M., Fattah, D., Solari, R., Peitsch, M. C., and Wells, T. N. (1995) *J. Biol. Chem.* **270,** 5762–5769
16. Tavernier, J., Tuypens, T., Verhee, A., Plaetinck, G., Devos, R., Van der Heyden, J., Guisez, Y., and Oefner, C. (1995) *Proc. Natl. Acad. Sci. U. S. A.* **92,** 5194–5198
17. Wu, S. J., Li, J., Tsui, P., Cook, R., Zhang, W., Hu, Y., Canziani, G., and Chaiken, I. (1999) *J. Biol. Chem.* **274,** 20479–20488
18. Bazan, J. F. (1990) *Proc. Natl. Acad. Sci. U. S. A.* **87,** 6934–6938
19. Somers, W., Ultsch, M., De Vos, A. M., and Kossiakoff, A. A. (1994) *Nature* **372,** 478–481
20. Walter, M. R. (2002) *BioTechniques* **33,** (suppl.) 46–57
21. Cornelis, S., Plaetinck, G., Devos, R., Van der Heyden, J., Tavernier, J., Sanderson, C. J., Guisez, Y., and Fiers, W. (1995) *EMBO J.* **14,** 3395–3402
22. Scibek, J. J., Evergren, E., Zahn, S., Canziani, G. A., Van Ryk, D., and Chaiken, I. M. (2002) *Anal. Biochem.* **307,** 258–265
23. Tavernier, J., Van der Heyden, J., Verhee, A., Brusselle, G., Van Ostade, X., Vandekerckhove, J., North, J., Rankin, S. M., Kay, B., and Robinson, D. S. (2000) *Blood* **95,** 1600–1607
24. Dowd, C. S., Leavitt, S., Babcock, G., Godillot, A. P., Van Ryk, D., Canziani, G. A., Sodroski, J., Freire, E., and Chaiken, I. M. (2002) *Biochemistry* **41,** 7038–7046
25. Myszka, G. D. (2000) *Methods Enzymol.* **323,** 325–340
26. Elkins, P. A., Christinger, H. W., Sandowski, Y., Sakal, E., Gertler, A., De Vos, A. M., and Kossiakoff, A. A. (2000) *Nat. Struct. Biol.* **7,** 808–815
27. Altschul, S. F., Madden, T. L., Schaffer, A. A., Zhang, J., Zhang, Z., Miller, W., and Lipman, D. J. (1997) *Nucleic Acids Res.* **25,** 3389–3402
28. Sali, A., and Blundell, T. L. (1993) *J. Mol. Biol.* **234,** 779–815
29. Devos, R., Guisez, Y., Plaetinck, G., Cornelis, S., Tavernier, J., Van der Heyden, J., Foley, L. H., and Scheffler, J. E. (1994) *Eur. J. Biochem.* **225,** 635–640
30. Laskowski, R. A., MacArthur, M. W., Moss, D. S., and Thornton, J. M. (1993) *J. Appl. Crystallogr.* **26,** 283–291
31. Sippl, M. J. (1993) *Proteins* **17,** 355–362
32. Luthy, R., Bowie, J. U., and Eisenberg, D. (1992) *Nature* **356,** 83–85
33. Plugariu, C. G., Wu, S. J., Zhang, W., and Chaiken, I. (2000) *Biochemistry* **39,** 14939–14949
34. Li, J., Cook, R., Dede, K., and Chaiken, I. (1996) *J. Biol. Chem.* **271,** 1817–1820
35. De Crescenzo, G., Pham, P. L., Durocher, Y., and O'Connor-McCourt, M. D. (2003) *J. Mol. Biol.* **328,** 1173–1183
36. Chaiken, M. I., and Proudfoot, E. I. A. (1999) in *Interleukin-5: From Molecule to Drug Target for Asthma* (Sanderson, C., ed) pp. 167–188, Marcel Dekker. Inc., New York
37. Czabotar, P. E., Holland, J., and Sanderson, C. J. (2000) *Cytokine* **12,** 867–873
38. Rajotte, D., Cadieux, C., Haman, A., Wilkes, B. C., Clark, S. C., Hercus, T., Woodcock, J. A., Lopez, A., and Hoang, T. (1997) *J. Exp. Med.* **185,** 1939–1950
39. Northrup, H. S., and Erickson, P. H. (1992) *Proc. Natl. Acad. Sci. U. S. A.* **89,** 3338–3342
40. Tello, D., Eisenstein, E., Schwarz, F. P., Goldbaum, F. A., Fields, B. A., Mariuzza, R. A., and Poljak, R. J. (1994) *J. Mol. Recognit.* **7,** 57–62
41. Freire, E. (1999) *Proc. Natl. Acad. Sci. U. S. A.* **96,** 10118–10122
42. Koradi, R., Billeter, M., and Wüthrich, K. (1996) *J. Mol. Graphics* **14,** 51–55
43. Thompson, J. D., Higgins, D. G., and Gibson, T. J. (1994) *Nucleic Acids Res.* **22,** 4673–4680